Heavy Metal Ion Detection on a Microspot Electrode Using an Optical Electrochemical Probe

Santanu Roy[†], Abhijeet Prasad[†], Rahul Tevatia, Ravi F. Saraf[*]

Department of Chemical and Biomolecular Engineering, University of Nebraska, Lincoln, NE 68588; [†]Equal contribution; *rsaraf2@unl.edu

Published in *Chemelectrochem* **2018**, 5 (3), 429-433

The manuscript below may be slightly different from the published MS.

Heavy Metal Ion Detection on a Microspot Electrode Using an Optical Electrochemical Probe

Santanu Roy[†], Abhijeet Prasad[†], Rahul Tevatia, Ravi F. Saraf[*]

Department of Chemical and Biomolecular Engineering, University of Nebraska, Lincoln, NE 68588; [†]Equal contribution; *rsaraf2@unl.edu

Abstract

Electrochemical sensors can be used to create portable, attractive, high-sensitivity devices to detect heavy ions in water at a reasonable cost. A novel method of measuring local redox on an electrode using the differential reflectivity measured on about 6 micron diameter spot using a He/Ne laser beam is described. Field focusing and electrode modification enhances the sensitivity, making the method ideal for miniaturization and multiplexing multiple analytes on a monolith electrode. The method is demonstrated by detecting Pb, Hg, and As ions at ppb and ppt levels.

Keywords: Heavy metals; electrochemical analysis; electrode size; dielectrophoretic effect; water pollution; electro-optics

1. Introduction

With ever-decreasing sources of water for the growing world population, the search for new sources and the recycling of water have made the issue of heavy metal ion contamination a ubiquitous problem and intensified the need for new detection systems, in terms of sensitivity, specificity, and portability. Toxicity of heavy metal ions is well documented [1-3] with several toxic metals, such as As, Cd, Pb, and Hg, having no known biological function [4]. Heavy metal ions are toxic to reproductive organs of females [5] and males [6], and some are also carcinogens [7]. Concentrations of Pb, Hg, and As in ppb levels a normal human body pose serious health hazards, such as plumbism, hypertension, emphysema, and even cancer with chronic, irreversible damage to organs such as kidneys, skeletal muscles, and soft tissues [8]. Highly sophisticated methods, such as inductively coupled plasma-mass spectroscopy (ICP-MS) have been developed to measure Cd, Hg, and Pb ions at a sensitivity of 4, 6, and 13 ppb, respectively [9]. Optical methods, such as atomic absorption spectroscopy (AAS), X-ray fluorescence spectroscopy (XRF), and inductively coupled plasma-optical emission spectroscopy (ICP-OES), have been developed to measure heavy metal ions at ppb levels [10, 11].

Arguably, electrochemical sensors are the most pervasive [11] with innovations in paper-based disposable devices [12] and enhanced sensitivity using nanomaterials [13-15] and biopolymers [16]. Apart from the simplicity and expense, electrochemistry is an attractive detection principle because the (redox current) signal is linearly proportional to the analyte concentration. However, the signal (and hence the sensitivity) diminishes as the size of the sensor is reduced. The modulation of the refractive index due to the change in ionic interface (i.e., electrical double layer (EDL)) during electrochemical reaction has also been leveraged by static [17] and dynamic [18] interferometry and

surface plasmon resonance [19,20]. Here, a simple optical technology based on differential reflectivity is described where the signal increases as the sensing area decreases to naturally decrease the device sensing size to micron levels. The principle of the method and its application for detecting Pb, Hg, and As ions at ppb levels is described.

2. Results and Discussion

The electrochemical reaction (of the redox moiety) was quantitatively probed by measuring the modulation in reflectivity of the sensing electrode due to the change in the interfacial ionic environment around the redox potential (Fig. 1(a)). The electrochemical system consisted of a standard three-electrode arrangement used in cyclic voltammetry (CV). The sensor's working electrode (WE) was made of bare Au in contact with a redox ion containing an aqueous solution. The reference electrode (RE) was Ag/AgCl, and Pt wire served as a counter electrode (CE). A potential, E, was applied between the RE and WE; and the current, I, was measured between WE and CE using a potentiostat (Autolab PGSTAT 128N). The WE was patterned with SU8 photoresist to expose a circular spot of diameter, d, ranging from 10 to 300 μm. Reflectivity of a He-Ne laser with a beam diameter of about 6 μm was measured from the WE during the CV. The reflectivity was measured as a differential signal by applying additional AC potential of frequency, ω = 0.5 kHz, on the WE. The reflected light intensity, R_A, modulated at ω due to ion oscillation caused by AC potential similar to that observed by differential interferometry [18, 21]. From the intensity of the constant reflected light, R_O, measured as a DC signal, differential reflectivity was obtained as, $R = R_A/R_O$. A typical signal for R as a function of multiple CV cycles from -0.1 to 0.6 V at a ramp rate of 0.5 V/s for 50 mM of $K_4[Fe(CN)_6]$ showed a highly periodic signal with excellent cycle-to-cycle reproducibility. About 75 scans in 3 minutes were obtained for analysis. For better visualization, magnified view of only a part of the data is shown to underscore the periodicity (Fig. 1(b)). Overlaying all of the cycles and filtering high frequency noise, the average signal, <R>, versus E with robust statistics, was obtained (Fig. 1(c)). The error-halo around <R> was the scatter due to cumulative cycle-to-cycle variations. Typically, the noise level at 500 Hz is less than 10^{-8}Ro. For no ions (i.e., blank), <R> is nominally a flat line implying that the signal is absolute.

The physical principle of the measurement is considered to relate R to (bulk) ion concentration, [c]. For normal beam, the reflectivity, r by Fresnel's law is, $r = |(N_1-N_2)/(N_1+N_2)|$, where N_1 and N_2 (=n-ik) are complex refractive index of the solution at the interface and metal, respectively. As the ion concentration in the EDL changes due to applied potential, N_1 ($=n_1-ik_1$) will modulate leading to change in r. Due to small AC potential at ω, the ion concentration at the interface will also oscillate at ω with an amplitude of δc_o. (In principle, ion modulation, δc will decrease as distance from electrode increases. For estimation, with no loss in formulation of the basic concept of the measurement, spatially averaged modulation, δc_o is considered). As differential refractive index, dn/dc is constant, for small AC potential, $n_1 = N + (dn/dc)\delta c_o \cos(\omega t)$, where, N is the refractive index at given E (i.e., equilibrium). The higher order oscillation of R_A at 2ω to 6ω measured by the lock-in amplifier is $>10^3$-fold smaller than R_A at ω. (The higher order effects may occur because of non-linear change in the ion concentration gradient as a function of distance from the electrode/solution interface.)

Assuming, the solution to be non-absorbing (i.e., $k_1 = 0$) and for Au, $n^2 << n_1^2$; and because the nonlinearity can be neglected (at 0.1% accuracy), the Fresnel's law for dynamic n_1 can be linerized to yield, |r| (at ω), $R = Q[(dn/dc)\delta c_o]\cos\omega t$, where $Q = [2n(N^2-k^2)/(N^2+k^2)]$.

Next relationship between E and δc_o is considered to relate the observed R_{max} to [c]. It is well known that, due to slow diffusion kinetics of ions during electrochemical reaction, there is a significant deviation from equilibrium of the ion concentration profile at the interface over a few microns [22]. As a result, the charge in the EDL significantly deviates from neutrality leading to insufficient screening causing a deeper penetration of the electric field emanating from the electrode. This maximization of oscillation of ion amplitude close to redox potentials due to the AC field is consistent with independent (and explicit) observation by differential interferometry [18,21]. Therefore, the reflectivity due to oxidation and reduction peaks at ${}^{o}R_{max}$ and ${}^{r}R_{max}$, respectively (Fig. 1(c)). At E far from the redox potential, δc_o is small leading to the small baseline (Fig. 1(c)). Furthermore, as ion diffusion is significantly slower than electron transport in the electrode, EDL discharge is linearly proportional to redox current which in turn is linearly proportional to bulk ion concentration, [c]. Thus, δc_o is linearly proportional [c]. Thus, after baseline subtraction, at the redox, $R_{max} = PQ[c]$, where P is a calibration constant that will depend on the dynamic properties of the target ions, such as diffusion constant and electrophoretic mobility that determines δc_o.

By scanning the laser beam and measuring R_{max}, local binding on a monolith electrode can be mapped. If the electrode were to be fabricated as a microarray of a local surface modification, multianalyte detection can be obtained. From known P, the target [c] can be quantified. Importantly, as the polarizability of the ion will change significantly due to its charge state of the ion, a large modulation in n_1 is expected, leading to high responsivity; while k_1 is nominally constant (as change in absorption at 633 nm is not large).

A typical <R> versus E for 50 mM showed a large variation in ${}^{o/r}R_{max}$ as a function of the patterned spot size, d. As shown by differential interferometry [21], the signal increased as d decreased due to field focusing (i.e., dielectrophoresis) (Fig. 2(a)). The signal was further enhanced as the thickness of the photoresist increased from 500 to 1200 nm (compare d = 50 μm for 500 and 1200 nm thickness in Fig. 2(a)). Conventional CV (not shown) indicated, as expected, the opposite effect where the peak oxidation current decreased from 50 μA to 20 μA as the size of the spot decreased from 300 μm to 50 μm due to a smaller electrode surface area. A systematic change in d showed the classic field focusing effect where the current density scales as 1/d (Fig. 2(b), inset) [23]. Because, the laser beam diameter was fixed, R_{max} corresponded to the current density rather than the total current [21]. The linear fit for 1/d versus R_{max} was excellent with a small intercept. The intercept of 0.46 corresponds to (limiting) signal for a large planar electrode. Thus, for a spot size of 50 μm and a thickness of 1200 nm, the enhancement due to field focusing relative to a large electrode was ~ 13-fold. For a larger thickness (i.e., 1200 nm in Fig. 2(b)), the signal began to decrease at a smaller d because of the incomplete etching during development of SU8 and the limitations of the lithography process (i.e., dishing effect). For a fixed [c] of 20 ppb, a similar size effect as $[Fe(CN)_6]^{4-/3-}$ is observed with a robust signal for Pb, Hg, and As for d = 50 μm. (Fig 2(c), data only

from the oxidation peak is shown). The signal is nominally enhanced by ~5-fold as the spot size is reduced from 300 to 50 μm at fixed thickness of 1200 nm.

The dielectrophoretic effect was leveraged to measure heavy metal ions (Fig. 3). The three ions tested were As (in As_2O_3), Hg (in $HgCl_2$), and Pb (in $PbCl_2$). The calibration curve for all the ions studied is highly linear with fitness of >0.95. The sensitivity to detect Pb ion is significantly enhanced by 3-folds by modifying the Au surface with adsorbed poly(styrene sulfonate) (PSS) (Fig. 3(a)). A robust peak is obtained at 50 ppt (Fig. 3(a), inset). The peak for a (baseline corrected) R_{max} of $0.17x10^{-4}$ is difficult to discern, leading to estimated limit of detection (LOD) of ~15 ppt. At ppb levels, the sensitivity of As ion in ppb levels is 1.5 levels lower than Pb on bare Au (Fig. 3(b)). By modifying the Au electrode with PSS and imbedding $[Ru(NH_3)_6]^{3+}$ ions using 32 cycle of CV ranging from -0.5 to 1.2 V, similar to a method described earlier [24], a robust peak is obtained at 1 ppt (Fig. 3(b), inset). Peak below 1 ppt is difficult to discern, leading to LOD of ~1 ppt. Sensitivity to detect Hg ion on bare Au was about 1.5 fold higher than Pb ion at ppb levels (Fig. 3(c)). By imbedding $[Fe(CN)_6]^{4-}$ ions on modified Au with PSS and poly(allylamine hydrochloride) PAH layers using the method described earlier [24], a robust peak is obtained at 1 ppt (Fig. 3(c), inset). For Hg, LOD was ~0.5 ppt corresponding to R_{max} of $\sim 0.068x10^{-4}$ (close to 1 ppt). All the ion detection was performed at d = 50 μm and resist thickness of 1200 nm. As indicated for Fig. 1(c), the signal with no ions (i.e., blank) for each modified electrode in the insets of Fig. 3 was zero indicating that R_{max} is an absolute measurement. The mechanism of the imbedded redox ion as described earlier [24], is to function as electron mediator to enhance the redox signal and thereby improve sensitivity. The error bar is calculated from the magnitude of the error halo at R_{max}. As the magnitude of the signal reduces, the width of the error halo also nominally reduces, however the relative error at low [c] is high as shown in the semilog plot (Fig. 3(d)). To demonstrate the quality of the signal averaged over 75 cycles, the inset of Fig. 3(a) to 3(c) shows the raw R with an error halo at the lowest [c] for each ion with no baseline correction. The potentials for R_{max} are consistent with the formal potentials of redox for As, Hg, and Pb ions which are at 320, 380, and 280 mV, respectively. Permissible safe levels of As, Hg, and Pb in drinking water set by the United States Environmental Protection Agency are 10, 10, and 15 ppb, respectively. Thus, the low LOD and strong signal at ppb levels in water demonstrates the feasibility of this approach to measuring the toxicity of heavy metal ions in water. Importantly, as multiple redox reactions can be measured on a monolith electrode, by locally modifying the electrodes, it will potentially be possible detect complex mixtures of heavy ions. The reasonableness of the signal (in Fig. 3) is inferred by estimating the ion modulation for measured R. To first order, the dn/dc will primarily be due to the anion owing to its (much) higher polarizability than the cation. Thus, for the chloride salts used in the study, dn/dc $\sim 10^{-1}$/M for Hg and Pb salts (based on NaCl). At equilibrium, $N \approx 1.4$ (the ions will raise the interfacial refractive index of water by ~10%). For Au (n = 0.18 and k = 3.07 at 633 nm) electrode, far from redox, $R \sim 0.5x10^{-5}$ leads to $\delta c_o \sim 2.5$ mM. For 500 ppb solution, $R \sim 10^{-4}$ at redox corresponds to δc_o of ~50 mM. Although the rise in concentration due to AC potential seems high, for [c] of 500 ppb (i.e., ~2 μM), the enhancement of $[Cl]^-$ in EDL(at equilibrium) at 200 to 300 mV electrode potential would be in 10^0 to 10^2 mM range from classical Poisson-Boltzmann distribution theory. Thus, the rough estimation of δc_o is reasonable within an order of magnitude. Furthermore,

consistent with the observation, for polyelectrolyte modified electrode n will increase and k will be lowered causing an increase of $[2n(N^2-k^2)/(N^2+k^2)]$ to make the electrode more sensitive.

3. Conclusions

In summary, the differential reflectivity method to measure current density is described where the signal enhances significantly due to field focusing effects and electrode modification. The signal is absolute. Limit of detection of 1 ppt is demonstrated for Hg and As ions, and 50 ppt for Pb ions. The calibration curve for all the three ions was highly linear over [c] ranging over five orders of magnitude. Furthermore, as the method measures local redox, potentially, multiple analytes on a monolith electrode can be detected by, for example, locally modifying the electrode surface with different polyelectrolytes and redox ions to develop a quantitative "artificial nose" to profile heavy metal ions.

References

[1] M. Jaishankar, T. Tseten, N. Anbalagan, B.B. Mathew, K.N. Beeregowda, Toxicity, mechanism and health effects of some heavy metals, Interdiscip. Toxicol. 7 (2014) 60-72.

[2] X. Wu, S.J. Cobbina, G. Mao, H. Xu, Z. Zhang, L. Yang, A review of toxicity and mechanisms of individual and mixtures of heavy metals in the environment, Environ. Sci. Pollut. Res. Int. 23 (2016) 8244-8259.

[3] H. Kozlowski, P. Kolkowska, J. Watly, K. Krzywoszynska, S. Potocki, General aspects of metal toxicity, Curr. Med. Chem. 21 (2014) 3721-3740.

[4] P.B. Tchounwou, C.G. Yedjou, A.K. Patlolla, D.J. Sutton, Heavy metal toxicity and the environment, EXS. 101 (2012) 133-164.

[5] P. Rzymski, K. Tomczyk, P. Rzymski, B. Poniedzialek, T. Opala, M. Wilczak, Impact of heavy metals on the female reproductive system, Ann. Agric. Environ. Med. 22 (2015) 259-264.

[6] J.J. Wirth, R.S. Mijal, Adverse effects of low level heavy metal exposure on male reproductive function, Syst. Biol. Reprod. Med. 56 (2010) 147-167.

[7] P. Koedrith, H. Kim, J.I. Weon, Y.R. Seo, Toxicogenomic approaches for understanding molecular mechanisms of heavy metal mutagenicity and carcinogenicity, Int. J. Hyg. Environ. Health. 216 (2013) 587-598.

[8] H. Schroeder, D. Darrow, Relation of trace metals to human health, Bost Coll Environ Aff Law Rev. 2 (1972) 222–236.

[9] H. Wang, Z. Wu, B. Chen, M. He, B. Hu, Chip-based array magnetic solid phase microextraction on-line coupled with inductively coupled plasma mass spectrometry for the determination of trace heavy metals in cells, Analyst. 140 (2015) 5619-5626.

[10] B.K. Bansod, T. Kumar, R. Thakur, S. Rana, I. Singh, A review on various electrochemical techniques for heavy metal ions detection with different sensing platforms, Biosensors and Bioelectronics. 94 (2017) 443-455.

[11] L. Pujol, D. Evrard, K. Groenen-Serrano, M. Freyssinier, A. Ruffien-Cizsak, P. Gros, Electrochemical sensors and devices for heavy metals assay in water: the French groups' contribution, Front. Chem. 2 (2014) 19.

[12] N.A. Meredith, C. Quinn, D.M. Cate, T.H. Reilly 3rd, J. Volckens, C.S. Henry, Paper-based analytical devices for environmental analysis, Analyst. 141 (2016) 1874-1887.

[13] P. Ramnani, N.M. Saucedo, A. Mulchandani, Carbon nanomaterial-based electrochemical biosensors for label-free sensing of environmental pollutants, Chemosphere. 143 (2016) 85-98.

[14] M. Govindhan, B. Adhikari, A. Chen, Nanomaterials-based electrochemical detection of chemical contaminants, RSC Adv. 4 (2014) 63741-63760.

[15] M. Li, H. Gou, I. Al-Ogaidi, N. Wu, Nanostructured Sensors for Detection of Heavy Metals: A Review, ACS Sustainable Chem. Eng. 1 (2013) 713-723.

[16] Y. Zhou, L. Tang, G. Zeng, C. Zhang, Y. Zhang, X. Xie, Current progress in biosensors for heavy metal ions based on DNAzymes/DNA molecules functionalized nanostructures: A review, Sensors and Actuators B: Chemical. 223 (2016) 280-294.

[17] Q. Li, H.S. White, Interferometric Measurement of Depletion Layer Structure and Voltammetric Data in Concentrated Organic Redox Solutions, Anal. Chem. 67 (1995) 561-569.

[18] G. Singh, D. Moore, R.F. Saraf, Localized Electrochemistry on a 10 um Spot on a Monolith Large Electrode: An Avenue for Electrochemical Microarray Analysis, Anal. Chem. 81 (2009) 6055-6060.

[19] D.G. Hanken, R.M. Corn, Electric Fields and Interference Effects inside Noncentrosymmetric Multilayer Films at Electrode Surfaces from Electrochemically Modulated Surface Plasmon Resonance Experiments, Anal. Chem., 69 (1997) 3665-3673.

[20] X. Shan, U. Patel, S. Wang, R. Iglesias, N. Tao, Imaging Local Electrochemical Current via Surface Plasmaon Resonance, Science, 327 (2010) 1363-1366.

[21] S.W. Lee, J. Lopez, R.F. Saraf, Direct mapping of local redox current density on a monolith electrode by laser scanning, Biosens. Bioelectron. 47 (2013) 408-414.

[22] R.G. Compton, C.E. Banks, Understanding Voltammetry, second ed., Imperial College Press, London, 2011.

[23] D.W. Arrigan, Nanoelectrodes, nanoelectrode arrays and their applications, Analyst. 129 (2004) 1157-1165.

[24] S.W. Lee, J. Lopez, R.F. Saraf, Fabrication and Properties of Redox Ion Doped Few Monolayer Thick Polyelectrolyte Film for Electrochemical Biosensors at High Sensitivity and Specificity, Electroanalysis. 25 (2013) 1557-1566.

a)

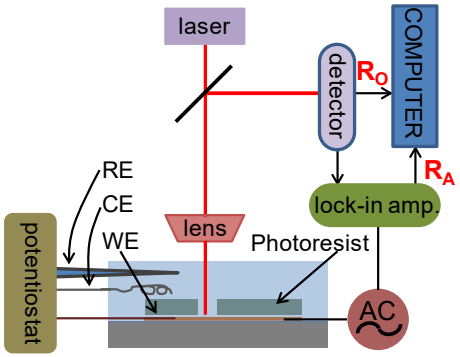

b)

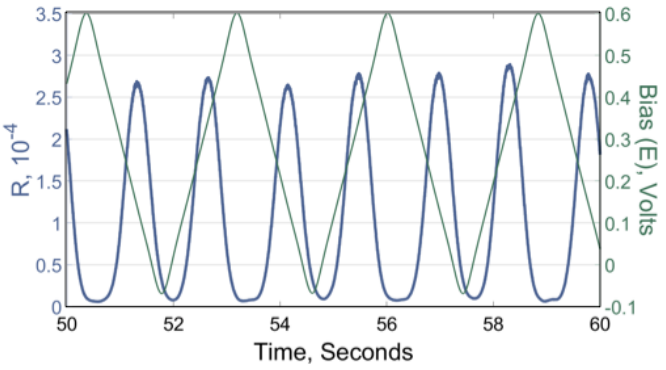

c)

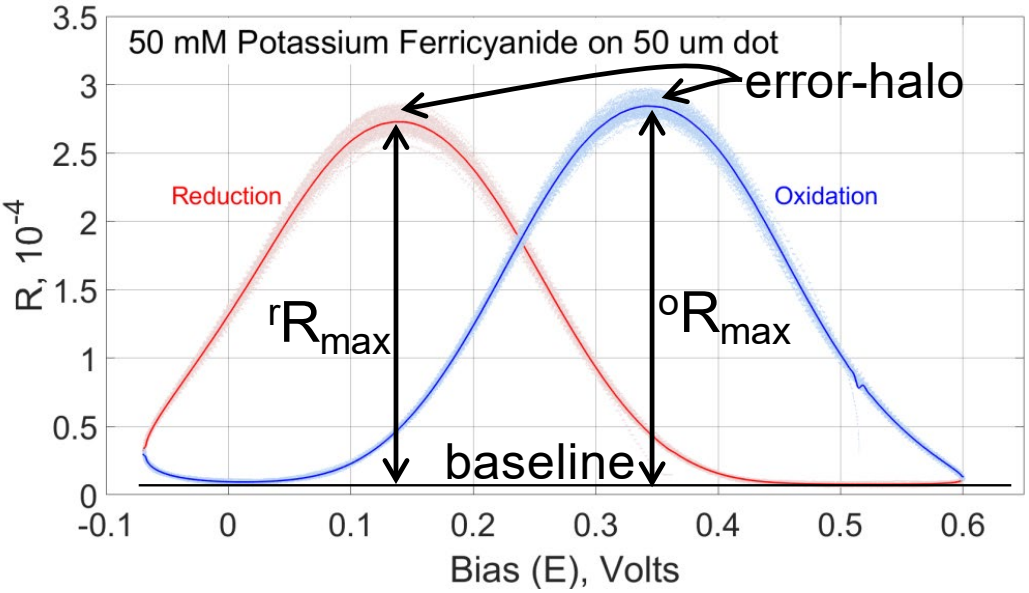

Figure 1. (a) Schematic displaying the optical set-up of the differential reflectometer. (b) Magnified scan of the raw data of reflectivity as a function of time showing highly repeatable redox peaks of $[Fe(CN)_6]^{4-/3-}$. (c) The <R> as a function of E by superposing about 75 scans from the raw data.

a)

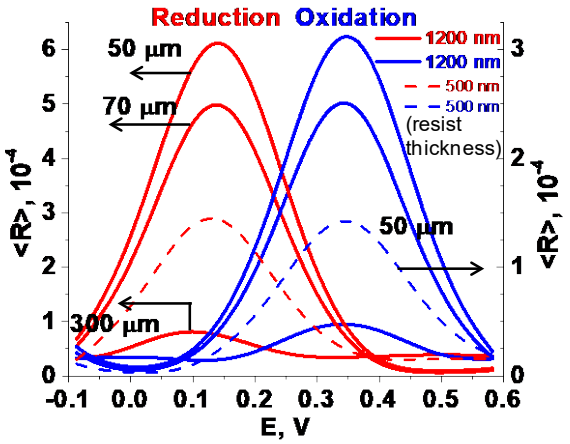

b)

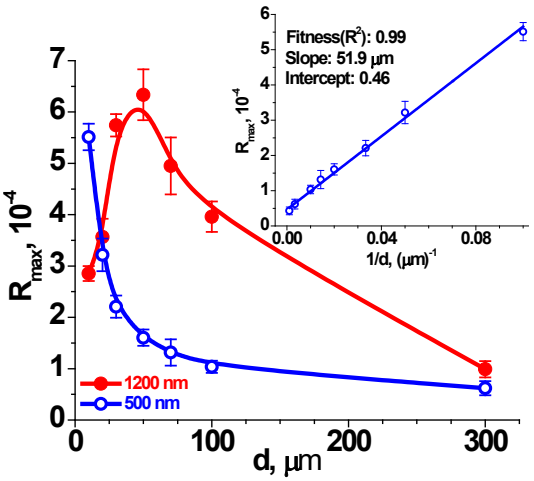

c)

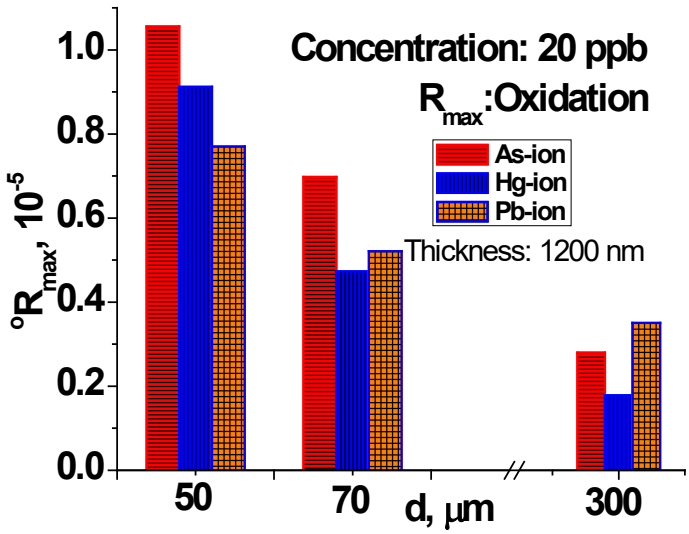

Figure 2. (a) Redox signal for 50 mM $K_4[Fe(CN)_6]$ as a function of resist thickness (nm) and the electrode diameter (□m). (b) R_{max} as a function of d for resist thickness of 1200 and 500 nm. Inset: Linear correlation of R_{max} versus 1/d for resist thickness of 500 nm. (c) The variation in R_{max} for heavy metal ions with d.

a)

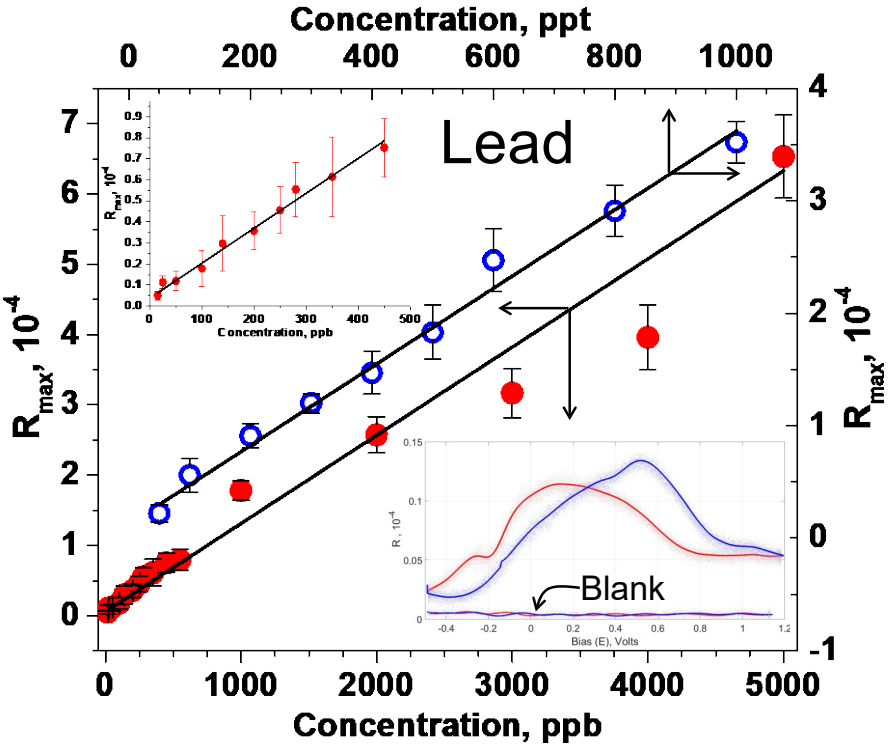
Concentration, ppt
0
200
400
600
800
1000
Lead
R_{max}, 10^{-4}
Concentration, ppb
0
1000
2000
3000
4000
5000
Blank
Bias (E), Volts

b)

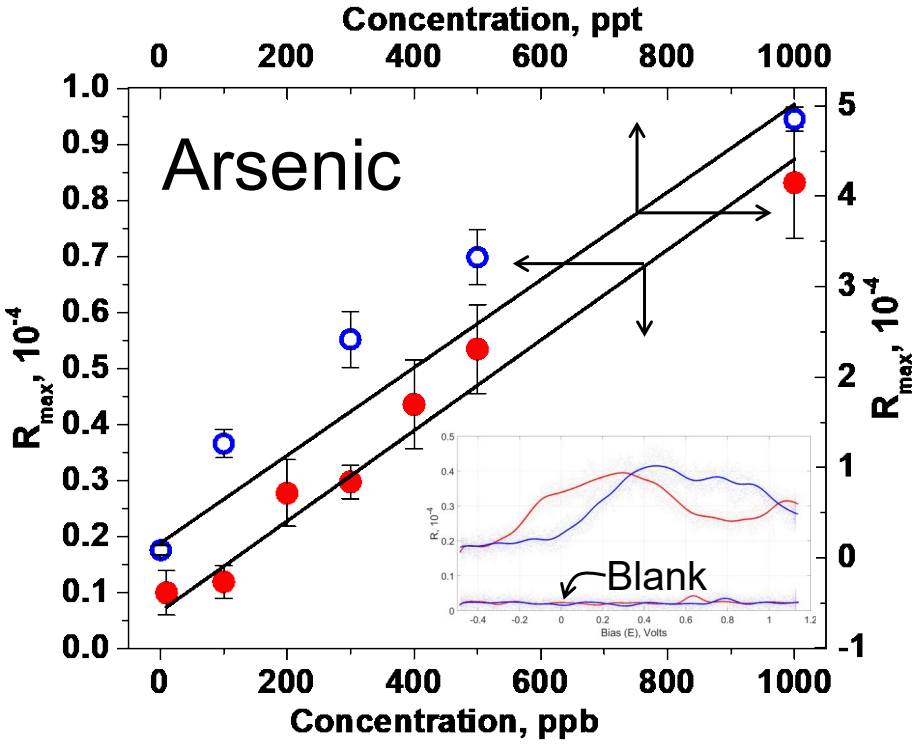
Concentration, ppt
0
200
400
600
800
1000
Arsenic
R_{max}, 10^{-4}
Concentration, ppb
Blank
Bias (E), Volts

c)

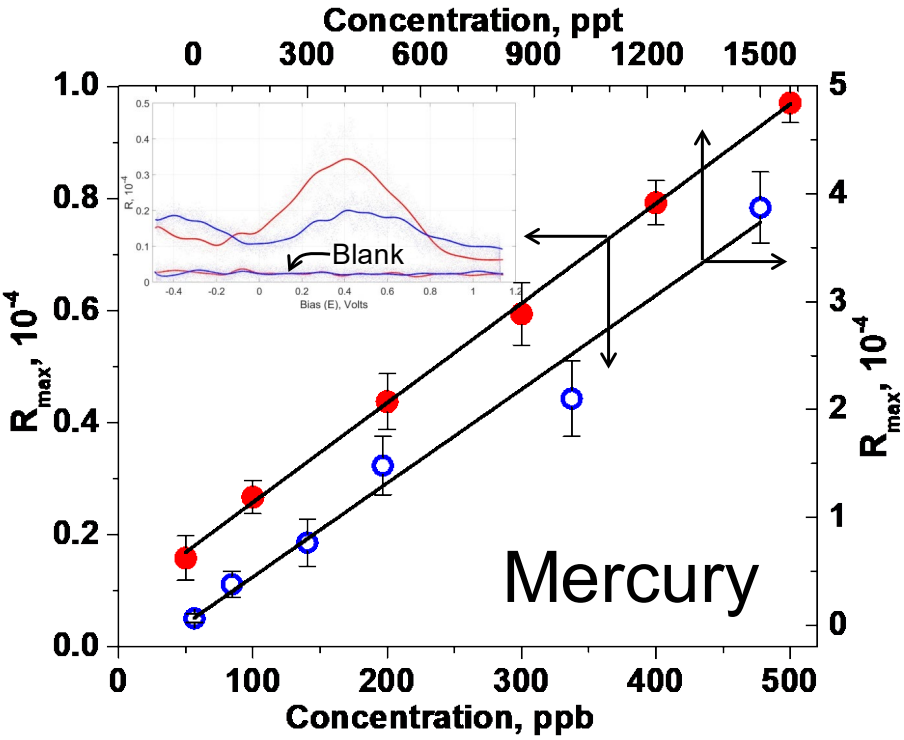

d)

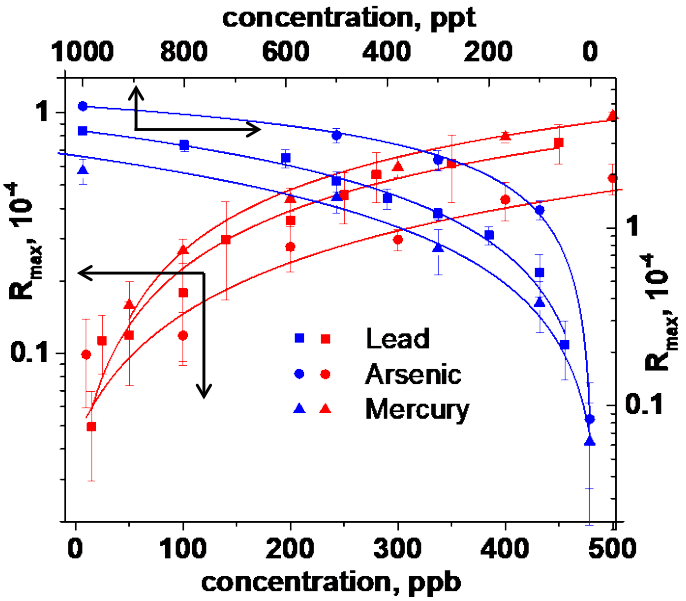

Figure 3. The calibration curve of heavy metal ions with linear relation between R_{max} and [c] (d= 50 and resist thickness = 1200 nm). (a) Pb on bare Au (ppb levels) and PSS modified Au (ppt levels). The responsivity (i.e., slopes) are 0.00125 and 0.00350 for the ppb and ppt levels, respectively. The inset shows raw data for 50 ppt Pb. (b) As on bare Au (ppb levels) and PSS modified Au with imbedded $[Ru(NH_3)_6]^{3+}$ ions (ppt levels). The responsivity are 0.00081 and 0.00486 for the ppb and ppt levels, respectively. The inset shows raw data for 1 ppt As. (c) Hg on bare Au microelectrode (ppb levels) and PSS and PAH modified with $[Fe(CN)_6]^{4-}$ ions (ppt levels). The responsivity are 0.00178 and 0.00245 for the ppb and ppt levels, respectively. The inset shows raw data for 1 ppt Hg. The blank in the insets is R to the corresponding modified electrode in distill water. (d) Semilog plot of calibration curves to show relative error.